JACS
JOURNAL OF THE AMERICAN CHEMICAL SOCIETY
Article
pubs.acs.org/JACS

High-Pressure Synthesis and Structural Characterization of the Type II Clathrate Compound $Na_{30.5}Si_{136}$ Encapsulating Two Sodium Atoms in the Same Silicon Polyhedral Cages

Shoji Yamanaka,*[,†] Masaya Komatsu,[†] Masashi Tanaka,[†] Hiroshi Sawa,[‡] and Kei Inumaru[†]

[†]Department of Applied Chemistry, Graduate School of Engineering, Hiroshima University, Higashi-Hiroshima 739-8527, Japan
[‡]Department of Applied Physics, Nagoya University, Nagoya 464-8603, Japan

Supporting Information

ABSTRACT: Single crystals of sodium containing silicon clathrate compounds Na_8Si_{46} (type I) and Na_xSi_{136} (type II) were prepared from the mixtures of NaSi and Si under high-pressure and high-temperature conditions of 5 GPa at 600−1000 °C. The type II crystals were obtained at relatively low-temperature conditions of 700−800 °C, which were found to have a Na excess composition $Na_{30.5}Si_{136}$ in comparison with the compounds Na_xSi_{136} ($x \leq 24$) obtained by a thermal decomposition of NaSi under vacuum. The single crystal study revealed that the Na excess type II compound crystallizes in space group $Fd\bar{3}m$ with a lattice parameter of a = 14.796(1) Å, slightly larger than that of the ambient phase ($Na_{24}Si_{136}$), and the large silicon hexakaidecahedral cages (@Si_{28}) are occupied by two sodium atoms disordered in the two 32e sites around the center of the @Si_{28} cages. At temperatures <90 K, the crystal symmetry of the compound changes from the face-centered to the primitive cell with space group $P2_13$, and the Na atoms in the @Si_{28} cages are aligned as Na_2 pairs. The temperature dependence of the magnetic susceptibility of $Na_{30.5}Si_{136}$ suggests that the two Na ions (2 Na^+) in the cage are changed to a Na_2 molecule. The Na atoms of $Na_{30.5}Si_{136}$ can be deintercalated from the cages topochemically by evacuation at elevated temperatures. The single crystal study of the deintercalated phases Na_xSi_{136} (x = 25.5 and 5.5) revealed that only excess Na atoms have disordered arrangements.

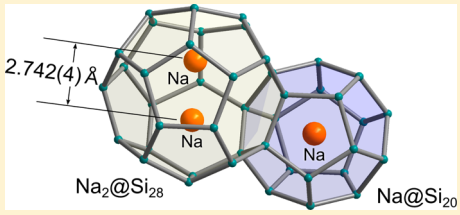

INTRODUCTION

The first silicon clathrate compounds Na_8Si_{46} (type I) and Na_xSi_{136} (type II) were prepared by the thermal decomposition of the Zintl compound NaSi by Kasper et al.[1] more than four decades ago. The compounds are isotypic with gas hydrates of the type I $G_x(H_2O)_{46}$ and the type II $G_x(H_2O)_{136}$ containing gas molecules (G), respectively. In silicon clathrate compounds the hydrogen bonds (H···OH) of the gas hydrates are replaced with Si−Si covalent bonds, and the silicon polyhedral cages encapsulate Na atoms instead of gas molecules. The type I silicon clathrate compounds are composed of face sharing 2 dodecahedral (Na@Si_{20}) and 6 tetrakaidecahedral (Na@Si_{24}) silicon cages per unit cell Na_8Si_{46}. The type II compounds are composed of face sharing 16 dodecahedral (Na@Si_{20}) and 8 hexakaidecahedral (Na@Si_{28}) silicon cages per unit cell $Na_{24}Si_{136}$ as shown in Figure 1. A variety of clathrate compounds with 14 group elements Si, Ge, and Sn in the framework have been prepared, whose frameworks are partially substituted with lower valent elements such as Ga, In, and Al.[2] The deficiency of the charge to complete octet arrangements for the covalently bonded framework is balanced by the electrons supplied from the encapsulated metal atoms in the cages. These charge-balanced clathrate compounds are called Zintl clathrate compounds.[3,4] There are a variety of combinations of the elements and the manners of substitution in the Zintl clatharate compounds, which can be usually prepared by a simple melting of the elemental mixture at ambient pressure and are considered to be potential candidates for thermoelectric materials.[5−7]

In the binary clathrate compounds such as Na_8Si_{46} and Na_xSi_{136}, electrons doped into the framework from metal atoms are extra; the Si atoms forming framework structures already have complete octets, and the extra electrons should be introduced into antibonding orbitals, i.e., the conduction bands. These kinds of compounds are called intercalation type clathrate compounds.[3,8] Most intercalation type clathrate compounds cannot be prepared by simple melting. The Na−Si clathrate compounds have been prepared by thermal decomposition of NaSi, and it was difficult to obtain single crystals. Recently, Nolas and his colleagues succeeded in obtaining single crystals of $Na_{24}Si_{136}$ by a controlled decomposition of NaSi using the formation of Na-graphite intercalation compound under spark plasma sintering.[9] The type I Na_8Si_{46} single crystals were also prepared in a niobium sealed tube by controlling Na vapor pressure in the thermal decomposition of NaSi.[10]

Ba_8Si_{46} is another example of a binary type I clathrate compound, which can be prepared only by using a high-pressure and high-temperature (HPHT) condition of 3 GPa at

Received: March 18, 2014
Published: May 1, 2014

   dx.doi.org/10.1021/ja502733e | J. Am. Chem. Soc. 2014, 136, 7717−7725

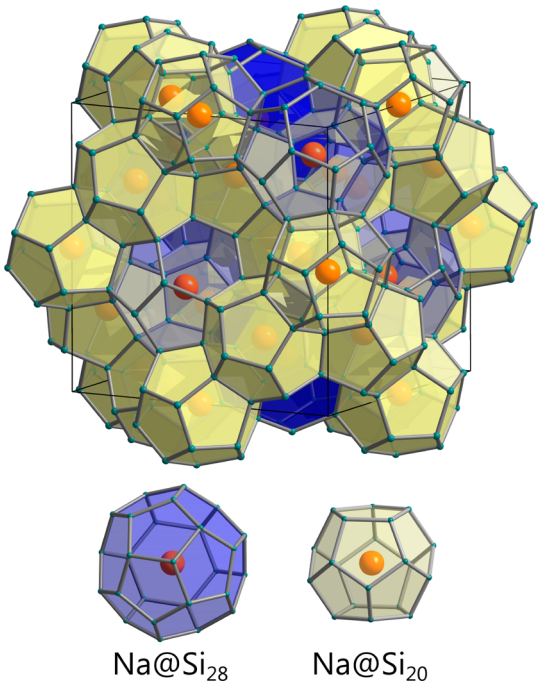

Figure 1. Schematic structural model of the type II (Na_xSi_{136}, $x \leq 24$) clathrate compound composed of 16 dodecahedra ($@Si_{20}$) and 8 hexakaidecahedra ($@Si_{28}$) per unit cell. Na atoms reside in the polyhedral cages.

800 °C.[11] Although it appears to be unusual to use high pressure for the synthesis of a cage-like compound, the volume change in the reaction system is calculated to be more than −16%, which appears to be the driving force of the formation of clathrate compound of intercalation type under high pressure.[11−13] Ba_8Si_{46} is a superconductor with a transition temperature of 8.0 K. In this study, Na−Si binary silicon clathrate compound is prepared using HPHT conditions. As the high-pressure effect, both type I and II clathrate compounds have been obtained as single crystals directly. In addition the type II crystals prepared in this study have an excess Na content $Na_{30.5}Si_{136}$ which has not been obtained by thermal decomposition of the Zintl compound NaSi. The crystal structures of the single crystals have been studied to reveal the distribution of the excess Na atoms in the cages. It has been found that two Na atoms are encapsulated in the same silicon polyhedral cages, $Na_2@Si_{28}$ analogous to dimetallofullerenes such as $La_2@C_{80}$ and $Sc_2@C_{84}$.[14,15] The temperature dependence of the magnetic susceptibility has been measured to estimate the nature of the Na atoms in the cages.

EXPERIMENTAL SECTION

High-Pressure Synthesis. Sodium monosilicide NaSi was first prepared by the reaction of Na metal and silicon powder loaded in a Ta crucible, which was sealed in a stainless steel tube using Swagelock sealing with Ar atmosphere, and heated at 450 °C for 3 days.[8] The resulting NaSi powder was mixed with Si powder in a molar ratio of 1:4 and filled in an h-BN cell (6 mm in inner diameter and 6 mm in depth) which was surrounded by a carbon tube heater and a zirconia thermal insulator tube. The whole sample assembly was centered in a pierced CoO-doped MgO octahedron as pressure medium and compressed using a Kawai-type multi-anvil press.[16] In most reactions, the high-pressure experiment was carried out at 5 GPa with various heating and cooling protocols. The starting mixtures of NaSi and Si were loaded in an Ar filled glovebox (MBRAUN).

Structural Characterization. Single crystals of the type II clathrate compounds were found and analyzed by SMART-APEX II (Bruker) and AFC7R Mercury (Rigaku) CCD diffractometers using MoKα radiation. The single crystal structure was refined with the program Shelx and the WINGX software package.[17,18] The data collection was performed at three different temperatures of 293, 90, and 10 K. The sample was also characterized by using an imaging plate Guinier diffractometer (Huber Model-670G) for powder sample. The single crystals were heated under vacuum to remove sodium at temperatures ranging from 300 to 450 °C. The structures of the single crystals of the type II compound with different compositions thus obtained were also analyzed in a similar way. The compositions of the clathrate crystals were determined by an electron probe micro analyzer (EPMA: scanning electron microscope Hitachi 3400, and EDAX Genesis XM2) using Na_8Si_{46} as standard.

Magnetic susceptibility was measured using a SQUID magnetometer (Quantum Design SQUID-VSM) in a temperature range of 2−300 K. The magnetic susceptibility was determined from the difference of the data measured at field strengths of 2000 and 5000 Oe to avoid the magnetic contamination effect. In order to estimate the structure of the clathrate compound with excess Na atoms theoretically, the structure was geometrically optimized using CASTEP ab initio program within the density functional theory (DFT) framework in Accelrys software suit.[19] The electronic band structure was calculated on the optimized crystal structure data. The calculations were carried out using the general gradient approximation, Perdew−Burke−Ernzehof (GGA-PBE) functional. Ultrasoft pseudopotentials were used within a plane wave basis with cut off energy of 370 eV.

RESULTS AND DISCUSSION

Preparation of Single Crystals. In a preliminary study for an HPHT condition, NaSi + Si mixture in a molar ratio of 1:4 was heated under 5 GPa and temperatures of 800−1000 °C for 20 min and rapidly cooled down to room temperature. The XRD study showed that the type I clathrate compound was obtained as single phase at 1000 °C, and the type II compound was formed at 800 °C as almost single phase with a small amount of Si. At 900 °C, a mixture of the two types of clathrate compounds was obtained. It is likely that higher reaction temperatures are favorable for the crystallization of the type I clathrate compound; the type II compound is obtained at lower temperatures. The HPHT treatment at 1 GPa at 1000 °C gave only a starting mixture of NaSi and Si, implying that a higher pressure is essentially required for the synthesis of the binary clathrate compounds. The molar volume differences in percent for the formation of the type I and the type II compounds are the following:

$$8NaSi + 38Si \rightarrow Na_8Si_{46}\ (Si/Na = 5.75) \quad -7.88\%$$

$$24NaSi + 112Si \rightarrow Na_{24}Si_{136}\ (Si/Na = 5.67) \quad -6.62\%$$

The two types of clathrate compounds have similar compositions, and the changes of the molar volumes in the formation reactions are also very close. It seems to be difficult to distinguish the formation of the two types of clathrate compounds by the pressure conditions. Fortunately, we can distinguish the formation conditions by the temperature.

The single crystals of the type II clathrate compound were obtained by the following thermal protocol; a molar mixture of NaSi + 4 Si was heated to 1000 °C for 10 min and then cooled down to 700 °C, where the mixture was kept for 1 h, followed by cooling to room temperature rapidly under a pressure of 5 GPa. The single crystals of the type I clathrate compound were obtained from the same molar mixture of NaSi + 4 Si, which was heated at 1000 °C for 1 h, followed by rapid cooling to room temperature under a pressure of 5 GPa.

dx.doi.org/10.1021/ja502733e | J. Am. Chem. Soc. 2014, 136, 7717−7725

Table 1. Lattice Parameters of the Type II (Na_xSi_{136}) and Type I (Na_8Si_{46}) Clathrate Compounds with Various Na Contents

composition	preparation condition	a, lattice parameter, Å	ref
$Na_{30.5}Si_{136}$	5 GPa, 700 °C	a = 14.796(1)[a]	this study
$Na_{25.5}Si_{136}$	deintercalation	a = 14.756(1)[a]	this study
$Na_{5.5}Si_{136}$	deintercalation	a = 14.647(1)[a]	this study
$1 < x < 20.5$, Na_xSi_{136}	thermal decomp.	14.6428(8) < a < 14.7030(5)	20
$Na_{24}Si_{136}$	spark plasma	a = 14.7157(2)[a]	21
$4.39 < x < 23.36$, Na_xSi_{136}	thermal decomp.	14.6196(3) < a < 14.70704(1)	22
$1.52 < x < 24.0$, Na_xSi_{136}	thermal decomp.	14.6465(5) < a < 14.7231(4)	8
Na_8Si_{46}	5 GPa, 1000 °C	10.2004(4)[a]	this study
Na_8Si_{46}	thermal decomp.	10.1973(1)[a]	21
Na_8Si_{46}	thermal decomp.	10.1983(2)	20
Na_8Si_{46}	thermal decomp.	10.19638(2)	22
Na_8Si_{46}	thermal decomp.	10.2037(1)	8

[a]Single crystal study.

Single Crystal Structures. Table 1 compares the compositions by EPMA and the lattice parameters of the single crystals obtained in this study with those reported in refs 8 and 20−22. It is known that the lattice parameter of the type II clathrate compound Na_xSi_{136} increases monotonically as the Na content x increases from a very low to a fully occupied compositions, as shown in the Table 1. The Na content of the type II clathrate compound obtained in this study was found to be x = 30.5, larger than that with the fully occupied composition, x = 24, and the lattice parameter (a = 14.790(1) Å) is slightly larger than that of $Na_{24}Si_{136}$ (a = 14.7157(2) ∼ 14.7228 Å) in literatures.[8,21,22] The Na excess composition, x > 24, suggests that 2 Na atoms should be encapsulated in the same silicon polyhedral cages. The type I clathrate compound obtained by HPHT synthesis has a stoichiometric composition Na_8Si_{46} and the lattice parameter (a = 10.2004(4) Å) is much the same as those prepared under ambient pressure by thermal decomposition of NaSi. The details of the single crystal structure investigations for $Na_{30.5}Si_{136}$ and Na_8Si_{46} at different temperatures are given in Table S1.

Recently, HPHT study on the Na−Si binary system has been reported by Kurakevych et al.[23] They reported that the type I clathrate Na_8Si_{46} was obtained by slow cooling from the 900−1000 K temperature range under a pressure ranging from 2 to 6 GPa, while a mixture of the type I and the type II $Na_{24}Si_{136}$ was obtained by a rapid quench to ambient temperature. They pointed out that the lattice parameter of the type II clathrate was 14.76(2) Å, expanded by ∼0.3% as compared to that of the compound obtained by thermal decomposition. However, no structural consideration was reported. When the pressure was increased to 8 GPa, they had a new binary compound $NaSi_6$. It has the $EuGa_2Ge_4$ structure isotypic with $BaSi_6$.[12,24]

Structure of $Na_{30.5}Si_{136}$ at Room Temperature (293 K). The crystallographic parameters of $Na_{30.5}Si_{136}$ at 293 K are shown in Table S2. It crystallizes in space group $Fd\bar{3}m$ with the lattice parameter a = 14.796(1) Å, slightly larger than that of the conventional Na_xSi_{136} (x < 24) with a = 14.62−14.72 Å as shown in Table 1.

A schematic illustration of the crystal structure is shown in Figure 2. In the unit cell 16 Na atoms (Na1) are placed at the center (16d site) of 16 small cages (@Si_{20}), and 14.5 Na atoms (Na2, Na21, and Na22) in the 8 large cages (@Si_{28}). This means that about 6 of 8 large cages in the unit cell are occupied by two Na atoms. As shown in the Figure 2, the two atoms

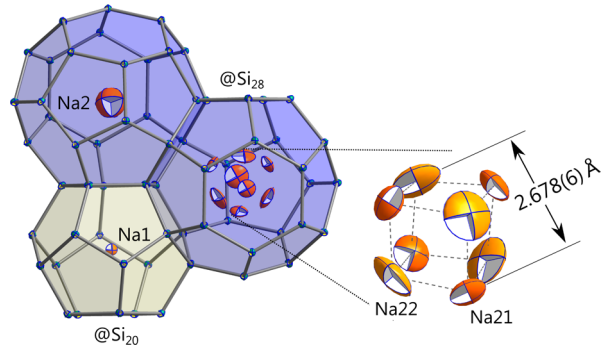

Figure 2. Schematic illustration of the crystal structure of $Na_{30.5}Si_{136}$ determined at 293 K. Anisotropic atomic displacement ellipsoids are shown at the 50% probability level. Two Na atoms (Na21 and Na22) are disordered in two kinds of 32e sites in the large polyhedral cages @Si_{28}. The two kinds of the disordered sites form a deformed cubic arrangement. The Na atoms (Na2) at the center of the large polyhedral cages represent the Na atoms placed singularly in the cage. To clarify the sizes of the atomic displacement ellipsoids, two cages are shown separately. In the structural analysis, Na atoms (Na2, Na21, and Na22) are overlapped in the same cages.

(Na21 and Na22) are distributed into two 32e sites, which form a deformed cube surrounding the 8a site at the center of the cage. The distance of the body diagonal of the cube is 2.678(6) Å. The atomic isotropic displacement parameter (U_{eq}) of Na1 (16d site) in @Si_{20} is as small as 0.0225(3) Å^2. The Na atoms (Na2) at the center of the large cages (8a site) represent the Na atoms placed in the large cage in single occupancy, which has a larger U_{eq} = 0.17(2) Å^2. The Na content (x) determined by the X-ray refinement without any restriction on the occupancy of the sites is determined to be x = 29.8, in good agreement with the EPMA composition $Na_{30.5}Si_{136}$.

We should note that Na21 atoms are located on the off-centered positions toward the center of the hexagonal faces of @Si_{28} cages. Since each @Si_{28} cage has four hexagonal faces and is tetrahedrally linked to four @Si_{28} cages by sharing the faces, all of the Na21 atoms on the four disordered sites (Figure 2) are facing to Na21 atoms from the adjacent @Si_{28} cages at a distance of 3.578(6) Å through the hexagonal window. This distance is close to the bond distance (3.079 Å) of Na_2 molecules in vapor phase determined by spectroscopic studies.[25] It has been reported for Na_8Si_{136}, in which all @Si_{28} cages are singularly occupied by Na atoms, that Na atoms are displaced by 0.9 ± 0.2 Å from the center of the cage toward

dx.doi.org/10.1021/ja502733e | J. Am. Chem. Soc. 2014, 136, 7717−7725

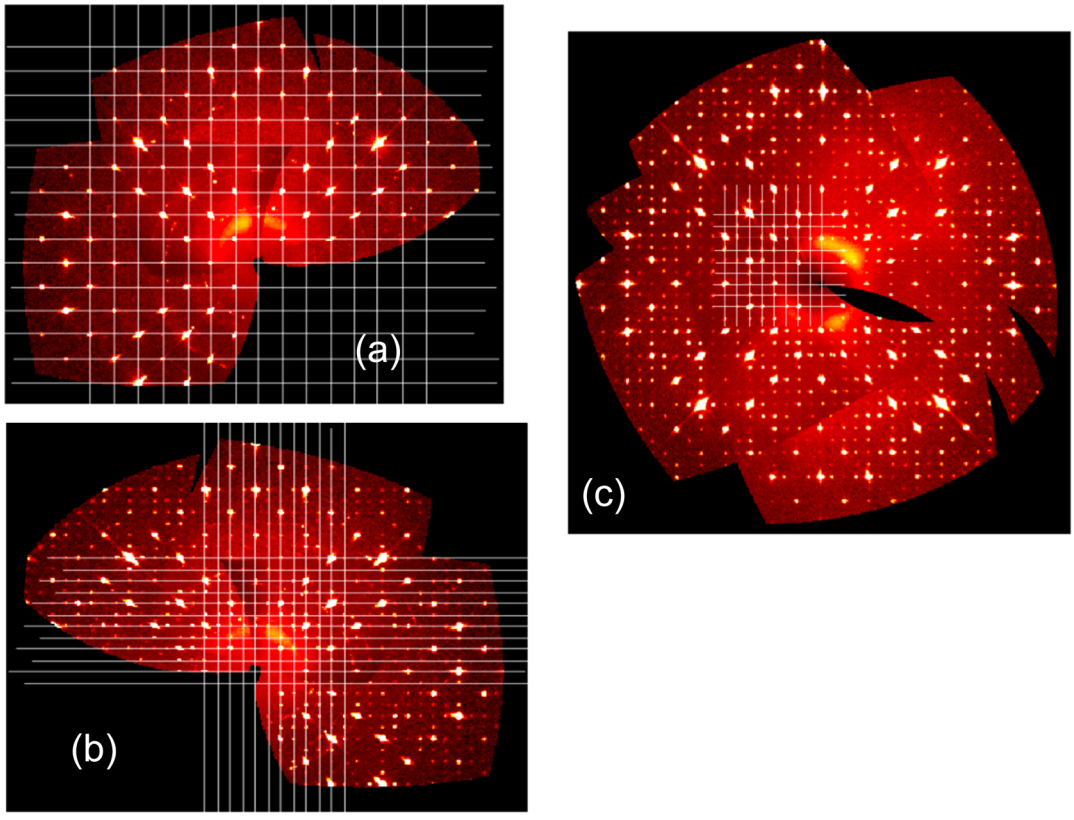

Figure 3. Precession images of the 0*kl* plane synthesized from the CCD single crystal diffraction data of $Na_{30.5}Si_{136}$ measured at (a) room temperature (hemisphere data collection), (b) 90 K (hemisphere data collection), and (c) 10 K (full sphere data collection). The space group of the crystal at room temperature is $Fd\bar{3}m$, and $P2_13$ at 90 and 10 K.

Table 2. Space Groups, SOF, and Isotropic Atomic Displacement Parameters U_{eq}s of the Clathrate Compounds with Different Compositions, Determined Based on the X-ray Reflection Data Collected at Different Temperatures

Formula	$Na_{30.5}Si_{136}$		$Na_{25.5}Si_{136}$		$Na_{5.5}Si_{136}$			$Na_{30.5}Si_{136}$		$Na_{30.5}Si_{136}$	
Temp., K	293		293		293			90		10	
a, Å	14.796(1)		14.756(1)		14.647(1)			14.768(1)		14.763(5)	
Sp. Group	$Fd\bar{3}m$		$Fd\bar{3}m$		$Fd\bar{3}m$			$P2_13$		$P2_13$	
Atom	SOF	U_{eq}, Å^2	SOF	U_{eq}, Å^2	SOF	U_{eq}, Å^2	Atom	SOF	U_{eq}, Å^2	SOF	U_{eq}, Å^2
Si1(8b)	1	0.0107(2)	1	0.015(7)	1	0.0121(4)	Si11(4a), Si12(4a)	1	0.0073(2)	1	0.0073(2)
Si2(32e)	1	0.0109(2)	1	0.0156(5)	1	0.0125(3)	Si21(4a), Si22(4a), Si23(12b), Si24(12b)	1	0.0074(1)	1	0.0071(1)
Si3(96g)	1	0.0110(1)	1	0.0157(4)	1	0.0121(2)	Si31(12b), Si32(12b), Si33(12b), Si34(12b), Si35(12b), Si36(12b), Si37(12b), Si38(12b)	1	0.0069(1)	1	0.0067(1)
Na1(16d) in $@Si_{20}$	1	0.0225(3)	1	0.0274(9)	0.06(1)	0.045(17)	Na11(4a), Na12(12b) in $@Si_{20}$	1	0.011(1) 0.0113(4)	1	0.010(1) 0.0094(4)
Na2(8a) in $@Si_{28}$	0.32(3)	0.17(2)	0.68(8)	0.128(18)	0.7(3)	0.166(9)	Na21(4a) in $@Si_{28}$(I)	0.363(3)	0.109(15)	0.39(3)	0.064(8)
Na21(32e) in $@Si_{28}$	0.169(5)	0.044(3)	0.06(2)	0.030(16)			Na22(4a) in $@Si_{28}$(I)	0.74(2)	0.016(2)	0.81(2)	0.013(1)
Na22(32e) in $@Si_{28}$	0.178(7)	0.076(5)	0.09(2)	0.090(32)			Na23(4a) in $@Si_{28}$(I)	0.66(2)	0.024(2)	0.68(2)	0.014(2)
							Na31(4a) in $@Si_{28}$(II)	0.28(2)	0.043(7)	0.17(2)	0.009(6)
							Na32(12b) in $@Si_{28}$(II)	0.25(1)	0.011(2)	0.26(1)	0.007(2)
							Na33(12b) in $@Si_{28}$(II)	0.25(1)	0.010(2)	0.29(1)	0.007(2)
x, $Na_x@Si_{20}$	16	Na total	16	Na total	0.96	Na total	*x*, $Na_x@Si_{20}$	16	Na total	16	Na total
x, $Na_x@Si_{28}$	13.8	= 29.8	10.2	= 26.2	5.6	= 6.6	*x*, $Na_x@Si_{28}$	14.2	= 30.2	14.8	= 30.8
Na found. (EPMA)		30.5		25.5		5.5	Na found (EPMA)		30.5		30.5

the center of the hexagonal faces. In a similar way, Na−Na pairs are formed in a distance of ∼4.34 Å through the shared hexagonal face. This was found by an extended X-ray absorption fine structure (EXAFS) spectroscopy[26] and supported by ab initio theoretical study.[27] The Na atoms in Na_8Si_{136} form a giant diamond lattice where each sodium atom

dx.doi.org/10.1021/ja502733e | J. Am. Chem. Soc. 2014, 136, 7717−7725

has four sodium neighbors at a distance of 6.34 Å. It is considered that a Peierls distortion assisted by the Jahn−Teller effect may induce the spin pairwise interactions in the giant sodium lattice. The disordered Na21 sites in @Si_{28} cages of this study also occupy the corresponding off-center sites facing to the center of the hexagonal rings, which are favorable to have a similar strong pairwise interaction with Na21 atoms of the next @Si_{28} cages, in addition to the interaction with Na22 at a shorter distance of 2.678(6) Å along the body diagonal of the disordered cuboid.

Structure of $Na_{30.5}Si_{136}$ Measured at 90 and 10 K. The crystal was analyzed at 90 and 10 K, and the results are shown in Tables S3 and S4, respectively. Precession photographs were constructed from the single crystal diffraction data. Figure 3 compares the reconstructed images of the 0*kl* layers at 293, 90, and 10 K. It is clearly shown that the face-centered lattice at 293 K is changed into a primitive cell at 90 and 10 K. The compound at 90 and 10 K crystallizes in space group $P2_13$ (No. 198), with a lattice parameter slightly smaller than that of 293 K due to a thermal shrinkage as shown in Table S1. The type II silicon clathrate compound at 293 K has space group $Fd\bar{3}m$, and has three kinds of crystallographically independent Si sites at 8b, 32e, and 96g (Si1, Si2, and Si3, respectively) as shown in Table 2. Although the crystal at 10 and 90 K with space group $P2_13$ has 14 kinds of independent Si sites, we assume that the Si atoms can be grouped into three kinds of subgroups corresponding to Si1, Si2 and Si3 sites of space group $Fd\bar{3}m$ as shown in Table 2, and the same atomic displacement parameters are assigned within the same subgroups. This can simplify the structural refinements, and can avoid negative atomic displacement parameters.

Figure 4 shows a schematic illustration of the structure of the face sharing large silicon polyhedral cages @Si_{28} with Na atoms in different kinds of distributions. The small silicon cages @Si_{20} (not shown here) are singularly occupied by Na atoms at the center. Note that there are two kinds of @Si_{28} cages containing

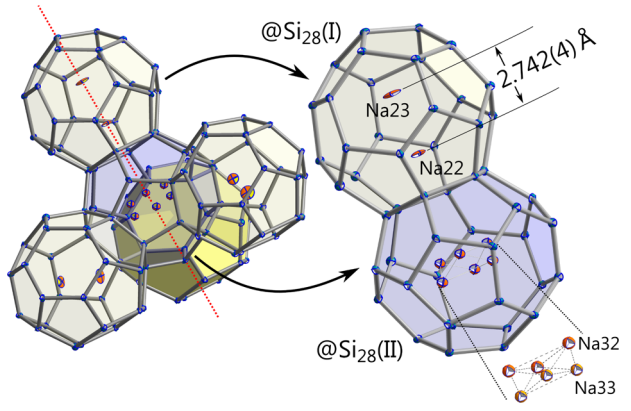

Figure 4. Schematic illustration of the crystal structure of $Na_{30.5}Si_{136}$ at 90 K. There are two kinds of large polyhedral cages @Si_{28}(I) and @Si_{28}(II) containing different distributions of Na atoms. Two Na atoms are encapsulated in each large cage as shown in the figure. Each cage is linked tetrahedrally by face sharing with the other kind of four large cages. In the large cage @Si_{28}(I), Na atoms (Na22 and Na23) form a pair and are aligned along the three-fold axis of the cage. The second large cage @Si_{28}(II) contains two Na atoms (Na32 and Na33) placed in disordered two sites. There are also large cages containing only one Na atom (Na21 or Na31) at the center of the cages (@Si_{28}(I) and @Si_{28}(II), respectively), which are not shown in the figure. Anisotropic atomic displacement ellipsoids are shown at the 80% probability level.

different kinds of Na distributions. Half of the @Si_{28} cages called @Si_{28}(I) contain two Na atoms as a pair which align along the three-fold axis of the crystal, and the other half of the @Si_{28} cages called @Si_{28}(II) contain two Na atoms distributed in a disordered way in two 12b sites forming a distorted octahedron. Each @Si_{28}(II) cage is tetrahedrally linked with four @Si_{28}(I) cages by sharing hexagonal rings and vice versa. As mentioned above, about 14 Na atoms are distributed into 8 @Si_{28} cages per unit cell, and about 2 of the 8 cages are singularly occupied by a Na atom. The Na atoms (Na21 and Na31) at 4a sites at the center of the @Si_{28} cages can be attributed to the singularly occupying atoms. The site occupancy factor (SOF) of each Na site was refined in the structural analysis without using any restriction condition. The total number of Na atoms at each site is listed in Table 2. The total numbers of Na atoms in @Si_{28}(I) and @Si_{28}(II) cages were determined to be 7.05 and 7.12, respectively. The total number of Na atoms in the @Si_{28} cages (14.2) is in good agreement with the number (13.8) found in the cages at room temperature. The Na atoms (Na21 and Na31) singularly occupying the cages are not shown in the figure, which are located at the center of the @Si_{28} cages. As shown in Table 2, the U_{eq}s for Na21 and Na31 are much larger than those of Na11 and Na12 located at the center of the smaller cages. The Na22 and Na23 atoms form a pair with a distance of 2.742(4) Å, slightly smaller than the distance (3.079 Å) determined for Na_2 molecules.[25] The molecular axis of the Na−Na pair is aligned along the three-fold axis running perpendicular to the hexagonal ring of the @Si_{28} cages, passing through the center of one of the four adjacent @Si_{28} cages (Figure 4). The structural analysis was also performed at a lower temperature of 10 K. However, the two structures are essentially the same as shown in Tables 2 and S4; only the atomic displacement parameters become smaller, and the distance between Na22 and Na23 has a slightly larger value of 2.766(4) Å. The larger distance is probably due to a smaller thermal interaction between the silicon cages and the confined Na−Na pairs at the lower temperature. The structural transformation from the face centered to the primitive cell appears to be completed at ~90 K.

As discussed on the structure of $Na_{30.5}Si_{136}$ at room temperature, the Na−Na distances belonging to the adjacent @Si_{28} cages are calculated based on the coordinates given in Table S3. The results are listed in Table 3. Each @Si_{28}(I) cage is tetrahedrally coordinated by four @Si_{28}(II) cages called [a], [b], [c], and [d] by sharing the hexagonal faces. The molecular axis of the Na22−Na23 pair in the @Si_{28}(I) cage passes

Table 3. Atomic Distances between Two Na Atoms Belonging to Two Adjacent @Si_{28} Cages Sharing the Hexagonal Faces in $Na_{30.5}Si_{136}$ at 90 K

Na in @Si_{28}(I)	Na in @Si_{28}(II)[a, b, c, d][a]	distance, Å
Na22	Na33[d] × 3	4.753(7)
↑	Na32[d] × 3	5.445(8)
2.742(4) Å	Na32[a], [b], [c]	5.643(8)
↓		
Na23	Na32[a], [b], [c]	4.700(8)
	Na33[a], [b], [c]	5.721(7)
	Na33[a], [b], [c]	5.881(7)

[a]The @Si_{28}(I) cage is tetrahedrally coordinated by four @Si_{28}(II) cages, [a], [b], [c], and [d] (see text).

dx.doi.org/10.1021/ja502733e | J. Am. Chem. Soc. 2014, 136, 7717−7725

through the center of the cage [d]. Na22 is bonded with Na23 at a short distance of 2.742(4) Å in the same @Si_{28}(I) cage and with Na32 × 3 and Na33 × 3 in [d] and Na32 × 3 in the other neighbors, [a], [b], and [c]. Note that Na23 atoms are also similarly coordinated by Na atoms in the three cages [a], [b], and [c] as shown in Table 3. It appears to be very strange that the disordered arrangement of Na atoms in @Si_{28}(II) is kept even at temperatures as low as 10 K. However, this arrangement would be one of the best solutions to have similar coordination environments for Na22 and Na23 atoms in the pair to stabilize the structure energetically.

Structure of $Na_{25.5}Si_{136}$ at Room Temperature. The Na excess compound is stable in ambient pressure even in air like Na_xSi_{136} (x < 24) and Na_8Si_{46}. The excess Na atoms can be removed by evacuation at elevated temperatures above 300 °C. The as-prepared single crystals $Na_{30.5}Si_{136}$ were evacuated at 300 °C for 1 h, and the structure was analyzed in a similar way. The composition was determined to be $Na_{25.5}Si_{136}$ by EPMA. The compound crystallizes with the same space group as $Na_{30.5}Si_{136}$ of $Fd\bar{3}m$. The structural analysis result is shown in Tables 2 and S5. The composition x > 24 suggests that there are still some Si cages encapsulating two Na atoms. The X-ray analysis shows that Na atoms in the large cages @Si_{28} are disordered, although most of Na atoms are at the center of the cages as shown in Table 2. The atomic displacement parameters are very similar to those of $Na_{30.5}Si_{136}$. It is very likely that only two Na atoms encapsulated in the same large cages have disordered arrangements.

Structure of $Na_{5.5}Si_{136}$ at Room Temperature. The as-prepared crystals were evacuated at 450 °C for 5 h and then analyzed in a similar way at room temperature. The composition was determined to be $Na_{5.5}Si_{136}$ by EPMA, and the single crystal analysis result is shown in Tables 2 and S6. In a previous study,[8] we analyzed the powder samples obtained by thermal decomposition of NaSi by the Rietveld method and showed that the Na atoms in Na_xSi_{136} are removed from the smaller cages (@Si_{20}) and then from the larger cages (@Si_{28}); the distribution of Na atoms can be estimated from the lattice parameter. Similar results have been reported by Ramachandran et al. and Reny et al.[22,23] The single crystal structural analysis of this study clearly shows that the population of Na atoms in the small cages is very low (0.96 Na atoms in 16 @Si_{20} cages) and that most Na atoms remain in the large cages (5.6 Na atoms in 8 @Si_{28} cages); the disorder distribution of the Na atoms in the large Si cages disappears. The U_{eq} for Na2 in the larger cage is 4 times larger than that of Na1 in the smaller cage.

Structure of Na_8Si_{46}. The structural analysis of the type I clathrate compound Na_8Si_{46} at room temperature is also shown in Table S7. The results are comparable with the single crystal data reported by Stefanoski et al.,[10] although they collected the X-ray intensity data at 200 K and obtained smaller atomic displacement parameters.

Magnetic Susceptibility. The temperature dependences of the magnetic susceptibilities of the type II ($Na_{30.5}Si_{136}$ and $Na_{24}Si_{136}$) and the type I (Na_8Si_{46}) compounds are compared in Figure 5. The magnetic susceptibilities of Na_8Si_{46} and $Na_{24}Si_{136}$ increase as the temperature decreases, in good agreement with those reported on the compounds with similar compositions.[28] The electrical properties of the Na−Si clathrate compounds have been well characterized in relation with the electronic structures.[28−31] Electron spin resonance (ESR) study of Na_3Si_{136} showed that the Na dopant states are located just below the conduction band of the silicon framework. At high

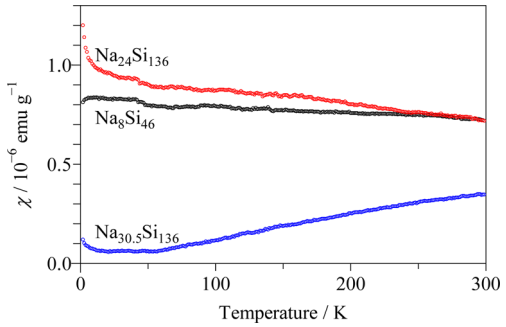

Figure 5. Temperature dependence of the magnetic susceptibility of silicon clathrate compounds: Na_8Si_{46} (black circle), $Na_{24}Si_{136}$ (red circle), and $Na_{30.5}Si_{136}$ (blue circle).

temperatures (T) with kT > 100 meV where k is the Boltzmann constant, the Na atoms are ionized, and the electrons are thermally excited into the framework bands. At low temperatures kT < ∼10 meV, the electrons become localized on the sodium atoms, producing a hyperfine signal.[3,32] In the clathrates with high Na contents Na_xSi_{136} with x > 20, the compounds do not exhibit an actual band gap at the Fermi level. The Pauli paramagnetic susceptibility and the Knight shift of the metallic Na_xSi_{136} clathrate compounds increase as the temperature decreases.

$Na_{30.5}Si_{136}$ shows a different temperature dependence on the magnetic susceptibility decreasing with decreasing temperature. The temperature dependence of the magnetic susceptibility shown in Figure 5 can be expressed using the following equation:

$$\Delta\chi = \chi(T) - \chi_0 \propto \exp(-\Delta E/kT)$$

where χ_0 is the susceptibility at ∼70 K, the temperature where no appreciable electron excitation is observed. $\Delta\chi$ is defined as $\chi_0 - \chi(T)$; $\chi(T)$ is the susceptibility at a measurement temperature and $\chi_0 = \chi$(70 K). The Arrhenius plot of the susceptibility difference $\Delta\chi$ gives a linear relationship as shown in Figure 6 and an activation energy of ΔE = 0.02 eV. Note that this temperature dependence of the magnetic susceptibility is similar to that found in Na_xSi_{136} with a low doping concentration (x = 3).[32] If we can assume the formation of neutral Na_2 pairs in @Si_{28} cages at low temperatures, the increase of localized electrons may decrease the Pauli magnetic

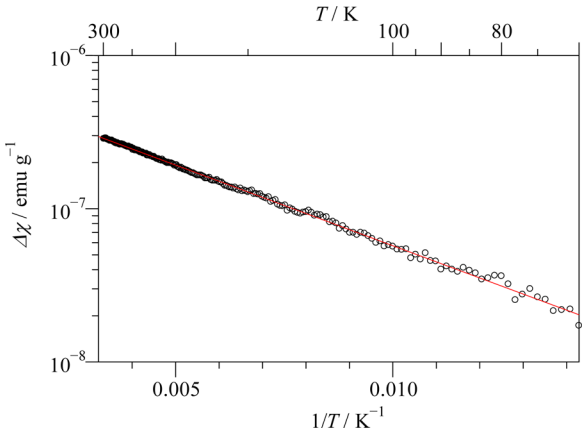

Figure 6. Arrhenius plot of the difference magnetic susceptibility ($\Delta\chi$) of $Na_{30.5}Si_{136}$ as a function of the reciprocal temperature.

dx.doi.org/10.1021/ja502733e | J. Am. Chem. Soc. 2014, 136, 7717−7725

susceptibility. The thermal excitation and ionization of the Na_2 pairs with an activation energy of 0.02 eV can explain the increase of the magnetic susceptibility with temperature as found in Figures 5 and 6.

Ab Initio Calculation. In order to estimate the effect of extra doping of Na atoms into $@Si_{28}$ cages, the electronic band structure of $Na_{32}Si_{136}$ was calculated. A structural model used for calculation is shown in Figure 7, where all of $@Si_{28}$ cages are fully occupied with Na_2 pairs, and $@Si_{20}$ cages are singularly fully occupied with Na atoms. The cell size is one-fourth of the full cubic cell with a formula unit of Na_8Si_{34}. The structure has space group $R\bar{3}m$ with the molecular axis of the Na−Na pair aligned along the three-fold axis. Although the model is different from a more realistic one containing disordered arrangements of Na atoms in $@Si_{28}$ cages, it should be useful to estimate the effect of the excess Na atoms in the same $@Si_{28}$ cages. The structure was geometrically optimized including the lattice parameters using CASTEP ab initio program.[19] The crystallographic parameters and the atomic coordinates obtained are given in Table 8S. The Na−Na distance of the pair is calculated to be 2.694 Å, comparable with the X-ray structural analysis value 2.766(4) Å (at 10 K). The optimized lattice parameters a = 10.5622 Å, and α = 59.3788° corresponds to a = 14.780 Å with a cubic structure in good agreement with the observed value (a = 14.763(5) Å) at 10 K.

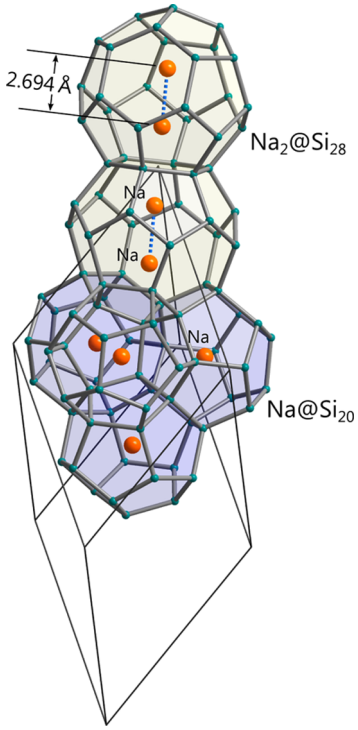

Figure 7. Structural model of $Na_{32}Si_{136}$ determined by geometrical optimization on the unit cell with space group $R\bar{3}m$; all of the large $@Si_{28}$ cages are filled with two Na atoms. The Na−Na distance is geometrically optimized to be 2.694 Å.

The electronic structures of Na_xSi_{136} with different compositions, x = 0, 4, 8, 16, and 24 have been systematically calculated by Smelyansky and Tse[31] to see the effect of the doping concentration on the electronic properties. Those compositions correspond to no doping (x = 0), half (x = 4), full (x = 8) occupancies of $@Si_{28}$ cages, full occupancy of $@Si_{20}$ cages (x = 16), and full occupancy of all of the cages (x = 24). Smelyansky and Tse showed that Na atoms in the two different kinds of cages have very different effects on the band structures. At a low doping concentration with x < 8, the lowest conduction band consists of predominantly Na 3s, and the contribution of Na 3p is very small. The electrons of Na atoms in $@Si_{28}$ cages are fairly localized in the narrow distribution of the density of states (DOS), and the clathrates are insulators. When the smaller $@Si_{20}$ cages are filled for a higher doping concentration, the total DOS indicates significant hybridization between Na (both 3s and 3p) and Si orbitals. The broad higher energy bands are partially filled with electrons, resulting in metallic conductivity. It is evident that the sodium clathrates cannot be regarded as ionic compounds with simple charge transfer from Na to the Si framework.

We have also calculated the total DOS and the partial DOS of Na atoms in $@Si_{20}$ and $@Si_{28}$ cages in $Na_{32}Si_{136}$ using the structural model shown in Figure 7. Similar DOS profiles were also calculated on Na_8Si_{136} and $Na_{24}Si_{136}$ to compare with the DOS of the present Na excess compound. The crystal data for Na_8Si_{136} and $Na_{24}Si_{136}$ were estimated from the single crystal data of $Na_{5.5}Si_{136}$ and $Na_{25.5}Si_{136}$ determined in this study with the Na occupancies being adjusted to Na_8Si_{136} and $Na_{24}Si_{136}$, respectively.

Figure 8 shows the total DOS and the partial DOS for the Na atoms in $Na_{32}Si_{136}$ in comparison with those of Na_8Si_{136} and $Na_{24}Si_{136}$. As described in the above paragraph, at a low Na concentration of x = 8, the lowest narrow band has predominantly Na 3s character, in good agreement with the result of Smelyansky and Tse.[31] In $Na_{24}Si_{136}$, the Fermi level moves upward for metallic conductivity; the broad conduction bands formed by the hybridization of Na (3s and 3p) and Si framework are partially filled with electrons. In $Na_{32}Si_{136}$ with excess Na atoms in $@Si_{28}$ cages, the partial DOS of Na atoms in $@Si_{20}$ is essentially unchanged from that in $Na_{24}Si_{136}$, while the partial DOS of Na in $@Si_{28}$ is significantly modified. As can be seen in Figure 8, the Na 3s of $@Si_{28}$ cages of $Na_{32}Si_{136}$ has another narrow distribution on the top of the conduction band, and the total DOS has a minimum near the Fermi level like a dip found in the DOS of the low doping clathrates Na_xSi_{136} (x < 8). Since the Na 3s electrons of $@Si_{28}$ cages in $Na_{32}Si_{132}$ are distributed near the top of the narrow conduction bands, the Na−Na pair formation is favorable at low temperatures. The pair formation is probably assisted by a spin−spin pairwise interaction as proposed by Brunet et al.[26] for the formation of Na_2 pairs in Na_8Si_{136} due to a Peierls−Jahn−Teller distortion in the giant diamond network of sodium.

■ CONCLUSIONS

The type II silicon clathrate compound with a Na excess composition $Na_{30.5}Si_{136}$ was obtained by the HPHT synthesis. The single crystal X-ray study revealed that two Na atoms are encapsulated in about 6 of 8 $@Si_{28}$ cages per unit cell and are disordered in two 32e sites (two kinds of 4 equiv positions) surrounding the center of the large cage $@Si_{28}$ at room temperature. At low temperatures <90 K, the two Na atoms in the same cages are ordered as Na−Na pairs with the molecular axis aligned along the three-fold axis of the crystal. This change induces the positive temperature-dependent Pauli paramagnetism. From the temperature dependence, the thermal activation energy for the ionization of a Na_2 pair to 2 Na^+ in the cages is estimated to be 0.02 eV. The Na_2 pair formation is probably due to a spin−spin pairwise interaction. The electronic band structure calculation also appears to support the pair formation.

dx.doi.org/10.1021/ja502733e | J. Am. Chem. Soc. 2014, 136, 7717−7725

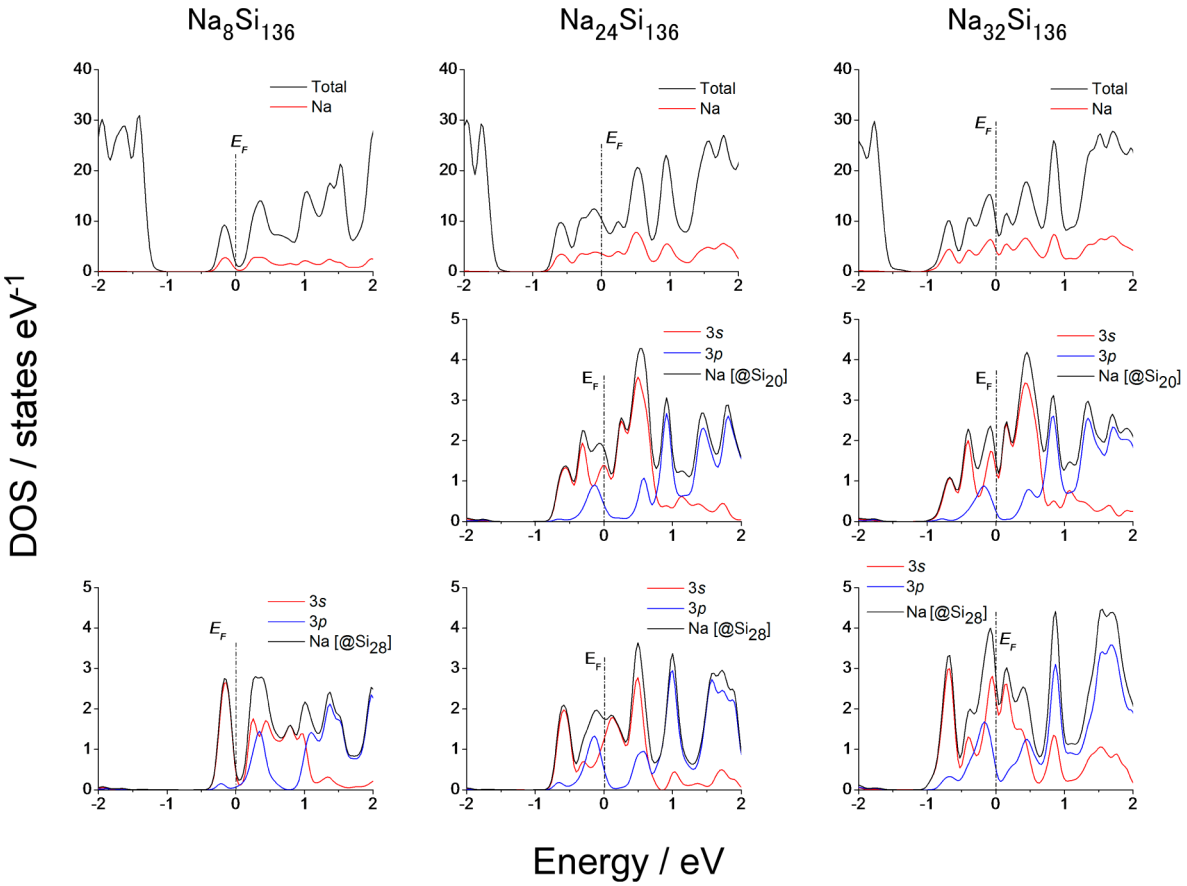

Figure 8. Total DOS (top panels) and the partial DOS of the Na atoms in @Si_{20} (middle panels) and @Si_{28} cages (bottom panels) of Na_8Si_{136}, $Na_{24}Si_{136}$, and $Na_{32}Si_{136}$.

Excess Na atoms can be removed by evacuation at elevated temperatures down to a composition of $Na_{5.5}Si_{136}$ through a singularly fully occupied composition $Na_{24}Si_{136}$. Disordered distributions of Na atoms disappear in the type II compounds with Na-deficient compositions with $x < \sim 24$ for Na_xSi_{136}.

■ ASSOCIATED CONTENT

Supporting Information

CIF files for the crystals listed in Table S1; $Na_{30.5}Si_{136}$ (293 K), $Na_{30.5}Si_{136}$ (90 K), $Na_{30.5}Si_{136}$ (10 K), $Na_{25.5}Si_{136}$, $Na_{5.5}Si_{136}$, and Na_8Si_{46}. These are available free of charge via the Internet at http://pubs.acs.org.

■ AUTHOR INFORMATION

Corresponding Author

syamana@hiroshima-u.ac.jp

Notes

The authors declare no competing financial interest.

■ ACKNOWLEDGMENTS

This work has been supported by the Japan Society for the Promotion of Science (JSPS) through its "Funding Program for World-Leading Innovative R&D on Science and Technology (FIRST) Program".

■ REFERENCES

(1) Kasper, J. S.; Hagenmuller, P.; Pouchard, M.; Cros, C. *Science* **1965**, *150*, 1713.
(2) Bobev, S.; Sevov, S. C. *J. Solid State Chem.* **2000**, *153*, 92.
(3) Pouchard, M.; Cros, C.; Hagenmuller, P.; Reny, E.; Ammar, A.; Ménétrier, M.; Bassat, J.-M. *Solid State Sci.* **2002**, *4*, 723.
(4) Yamanaka, S. *Dalton Trans.* **2010**, *39*, 1901.
(5) Slack, G. A. *Mater. Res. Soc. Symp. Proc.* **1997**, *478*, 47.
(6) Nolas, G. S.; Cohn, J. L.; Slack, G. A.; Schujman, S. B. *Appl. Phys. Lett.* **1998**, *73*, 178.
(7) Christensen, M.; Johnsen, S.; Iversen, Bo B. *Dalton Trans.* **2010**, *39*, 978.
(8) Horie, H.; Kikudome, T.; Teramura, K.; Yamanaka, S. *J. Solid State Chem.* **2009**, *182*, 129.
(9) Beekman, M.; Baitinger, M.; Borrmann, H.; Schnelle, W.; Meier, K.; Nolas, G. S.; Grin, Y. *J. Am. Chem. Soc.* **2009**, *131*, 9642.
(10) Stefanoski, S.; Beekman, M.; Wong-Ng, W.; Zavalij, P.; Nolas, G. S. *Chem. Mater.* **2011**, *23*, 1491.
(11) Yamanaka, S.; Enishi, E.; Fukuoka, H.; Yasukawa, M. *Inorg. Chem.* **2000**, *39*, 56.
(12) Yamanaka, S.; Maekawa, S. *Z. Naturforsch. B* **2006**, *61*, 1493.
(13) San-Miguel, A.; Toulemonde, P. *High Pressure Res.* **2005**, *25*, 159.
(14) Nagase, S.; Kobayashi; K., Akasaka; T.; Wakahara, T.; In *Fullerenes Chemistry, Physics and Technology*, Kadash, K. M., Ruoff, R. S., Eds; Wiley Interscience: New York, 2000; Chapter 9.
(15) Popov, A. A.; Yang, S.; Dunsch, L. *Chem. Rev.* **2013**, *113*, 5989.
(16) Kawai, N.; Endo, S. *Rev. Sci. Instrum.* **1970**, *41*, 1178.
(17) Sheldrick, G. *Acta Crystallogr.* **2008**, *64*, 112.
(18) Farrugia, L. *J. Appl. Crystallogr.* **1999**, *32*, 837.
(19) *CASTEP* Ver. 6.0; Accelrys: San Diego, CA (http://www.accelrys.com). Clark, S. J.; Segall, M. D.; Pickard, C. J.; Hasnip, P. J.; Probert, M. J.; Refson, K.; Payne, M. C. *Z. Kristall.* **2005**, *220*, 567.
(20) Reny, E.; Gravereau, P.; Cros, C.; Pouchard, M. *J. Mater. Chem.* **1998**, *8*, 2839.
(21) Beekman, M.; Nolas, G. S. *J. Mater. Chem.* **2008**, *18*, 842.

(22) Ramachandran, G. K.; Dong, J.; Diefenbacher, J.; Gryko, J.; Marzke, R. F.; Sankey, O. F.; McMillan, P. F. *J. Solid State Chem.* **1999**, *145*, 716.
(23) Kurakevych, O. O.; Strobel, T. A.; Kim, D. Y.; Muramatsu, T.; Struzhkin, V. V. *Cryst. Growth Des.* **2013**, *13*, 303.
(24) Bryan, J. D.; Stucky, G. D. *Chem. Mater.* **2001**, *13*, 253.
(25) Babaky, O.; Hussein, K. *Can. J. Phys.* **1989**, *67*, 912.
(26) Brunet, F.; Mélinon, P.; San Miguel, A.; Kéghélian, P.; Perez, A.; Flank, A. M.; Reny, E.; Cros, C.; Pouchard, M. *Phys. Rev. B* **2000**, *61*, 16550.
(27) Libotte, H.; Gaspard, J.-P.; San Miguel, A.; Mélinon, P. *Europhys. Lett.* **2003**, *64*, 757.
(28) Latturner, S.; Iversen, Bo B. *Phys. Rev. B* **2001**, *63*, 125403.
(29) Mott, N. F. *J. Solid State Chem.* **1973**, *6*, 348.
(30) Gryko, J.; McMillan, P. F.; Marzke, R. F.; Dodokin, A. P.; Demkov, A. A.; Sankey, O. F. *Phys. Rev. B* **1998**, *57*, 4172.
(31) Smelyansky, V. I.; Tse, J. S. *Chem. Phys. Lett.* **1997**, *264*, 459.
(32) Yahiro, H.; Yamaji, K.; Shiotani, M.; Yamanaka, S.; Ishikawa, M. *Chem. Phys. Lett.* **1995**, *246*, 167.